TASK ORIENTED OPTIMAL GRASPING BY MULTIFINGERED ROBOT HANDS

by

Zexiang Li and Shankar Sastry

Memorandum No. UCB/ERL M86/43

30 May 1986

TASK ORIENTED OPTIMAL GRASPING BY MULTIFINGERED ROBOT HANDS

by

Zexiang Li and Shankar Sastry

Memorandum No. UCB/ERL M86/43

30 May 1986

ELECTRONICS RESEARCH LABORATORY

College of Engineering
University of California, Berkeley
94720

TASK ORIENTED OPTIMAL GRASPING BY MULTIFINGERED ROBOT HANDS

by

Zexiang Li and Shankar Sastry

Memorandum No. UCB/ERL M86/43

30 May 1986

ELECTRONICS RESEARCH LABORATORY

College of Engineering
University of California, Berkeley
94720

Task Oriented Optimal Grasping by Multifingered Robot Hands

By *Zexiang Li** and *Shankar Sastry**

Electronics Research Laboratory and
Department of Electrical Engineering & Computer Sciences
University of California, Berkeley, CA.94720

ABSTRACT

This paper discusses the problem of optimal grasping of an object by a multifingered robot hand. We axiomatize using screw theory and elementary differential geometry the concept of a grasp and characterize its stability. Three quality measures that can be used to evaluate a grasp are then proposed. The last quality measure is task oriented and needs the development of a procedure for modeling tasks as ellipsoids in wrench space of the object. Numerical computation of these quality measures and the selection of an optimal grasp are addressed in detail. Several examples are given using these quality measures to show that they are consistent with human grasping experience.

This research is supported by NSF PYI Grant #DMC 8451129. The authors would like to thank Drs. Robyn Owens, Brad Paden and Mr. John Hauser, Paul Jacobs and Greg Heinzinger for their critical and useful comments.

Table of Contents

Task Oriented Optimal Grasping by Multifingered Robot

*Zexiang Li** and *Shankar Sastry**

Electronics Research Laboratory and

Department of Electrical Engineering & Computer Sciences

University of California, Berkeley, CA. 94720

1. Introduction

There has long been an interest in understanding dextrous multifingered robot hands. The interest arises not only from the desire to increase the flexibility of the current generation industrial robot systems but also from the hope of improving prosthetic devices for humans that have either partially or completely lost their limb control (see for example Jacobsen etal [23]). In most industry applications, the advantage of multifingered, dextrous robot hand over the existing two fingered parallel-jaw grippers is apparent. Stacking an array of special purpose grippers as proposed in [6] is not only cumbersome but also costly. The versatility of the human hand demonstrates a good example of using a multifingered dextrous hand in stead of the simple two fingered hand, even though it is still not an ideal hand as pointed out by Cutkosky [6].

1.1 The Problem of Grasping

Once a multifingered robot hand has been built, one of the most basic questions to be answered is the determination of grasps. Namely, given an object together with a task to perform, what is the appropriate grasp of the object so that the task can be executed efficiently? During the process of selecting grasps, will the task or shape and size of the object dictate the grasp, or will stable grasps always tell the full story and in such situations how does one find the stable grasps? While the question is

This research is supported by NSF PYI Grant #DMC 8451129. The authors would like to thank Drs. Robyn Owens, Brad Paden and Mr. John Hauser, Paul Jacobs and Greg Heinzinger for their critical and useful comments.

answered by many authors ([3], [5], [10], [20] & [21]) using stability as the unique measure, no satisfactory answer to the former question is available yet. It is our goal in this paper to aim at these problems.

1.2 Previous Work

Here we summarize previous work in the field.

In [10], Lozano Perez studied grasping based on three principal considerations: *safety*, *reachability*, and *stability*. While stability of a grasp is understood from its own context, by safety it is meant that the robot must be safe at the initial and final grasp configuration, and by reachability it is meant that the robot must be able to reach the initial grasp configuration, and with the object in hand, to find a collision-free path to the final grasp configuration.

In Hanafusa and Asada [3], a potential function approach was used to study stable prehension by a robot hand with elastic fingers. It was concluded that a grasp was stable if and only the potential function was at its minimum at the grasp configuration.

In Salisbury [5], screw theory was used to construct the grasp matrix of a grasp. The author reasoned that algebraically a grasp would be stable if and only if the grasp matrix had full row rank. Unisense forces were handled in [5] by requiring a sufficient number of internal forces. The work of [5] does not generalize readily to the finite frictional force case.

Kerr in [7] extended the work of [5] to include finite frictional forces in the study of grasp stability. The role of internal grasp forces was carefully studied in [7] and an optimality condition of applying internal forces to grasped objects was presented.

Quasi-static analysis was used in Jameson [9] to predict grasp stability. A goal grasping function was developed, which was used as an optimization criterion for selecting a set of grasping points.

In [6] Cutkosky extensively examined human grasping and concluded that the choice of grasp was dictated less by the size and shape of the object than by the tasks to be performed with the object. In other words, an optimal grasp needed to be task oriented. Various classes of human grasps were carefully illustrated in [6] to inspire the study and design of a robot hand.

The authors of [19] and [21] have studied automatic generation of gripping positions for a simple two-fingered parallel-jaw gripper. Several grasping quality measures were proposed in [19] and a single measure that combined these measures was used to evaluate a grasp. The optimal grasp according to [19] was the one that achieves the highest rating. Peshkin and Sanderson [21] describe an algorithm that generates a set of grasping points on a polygonal object for a two fingered hand.

1.3 Unsolved Problems and Our Contribution

Most of the previous work ([3], [5], [7], [8], [9], [19] & [21]) has concentrated on stability aspects of a grasp, and optimal stable grasps. They do not however take into account individual task requirement.

Cutkosky in [6] first included task requirements in selecting grasps. But he did not give the technical details as to how to incorporate task requirements into this selection process, and the question of how to determine the optimal task oriented grasp under certain constraints was not answered.

Undoubtedly, the ability to determine a grasp which is optimal with respect to the task to be performed facilitates the understanding and designing of a dextrous and versatile robot hand. While the human hand can select the optimal task oriented grasp without any difficulty, it is an extremely complicated process for the robot hand. To complete this mission, it is necessary that we understand well the following sub-problems:

(1). Modeling of the hand: how many contacts are allowed per finger and where should the contacts occur, at the finger links or at the fingertips?

(2). What contact structures and what extra assumptions are made on the hand?

(3). How does one systematically characterize grasping stability (such as the approaches taken by [5] & [7])?

(4). How does one model a task and the robot working environment?

(5). How does one incorporate this task modeling into a grasping quality measure? With this quality measure how does one determine the optimal grasp subject to various constraints?

In this paper, we present an approach for solving these subproblems: A brief outline of this paper is as follows:

In Section 2 we axiomatize and formalize using screw theory and some elementary differential geometry the concept of a grasp by a multifingered robot hand. The definitions are broad enough to cover both unisense and finite friction force contacts for a large number of commonly encountered contacts. Using this formalism we study and characterize the stability of a grasp.

In Section 3, we give three different quality measures for grasping: a minmax, or worst case quality measure δ, a volumetric measure ν and finally our task oriented measure μ. The development of the task oriented measure μ requires the modeling of tasks. We also discuss numerical computation of the quality measures. We have developed software to perform these calculations and a few sample applications of this software are presented in the text of the paper. Further, we discuss the calculation of optimal grasping (optimal in the sense of optimizing μ, ν, or δ). Finally, we make some comments on grasping constraints imposed by oddly shaped objects, fine manipulation and dynamic questions on grasping.

In Section 4 we collect some suggestion for future work.

2. Rigid Body Dynamics and Grasping Structures

2.1. Rigid Body Dynamics

Consider a rigid body B in R^3. Let X-Y-Z be an arbitrarily chosen inertial frame and x-y-z be a coordinate frame attached to the body.

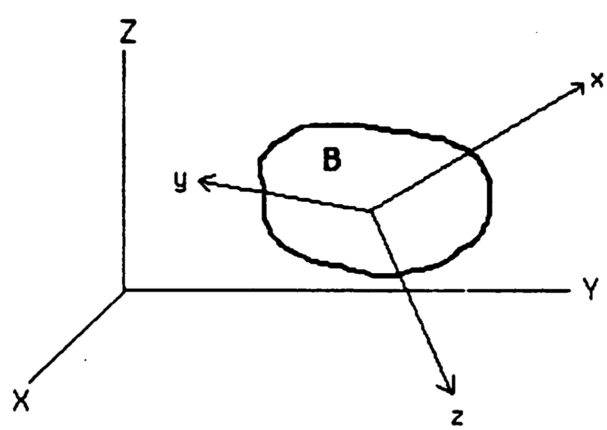

Figure 1. Rigid body in R^3 space.

The instantaneous configuration of the rigid body can be described by the orientation and the position of the body frame x-y-z in terms of the inertial frame X-Y-Z. We define the configuration space (or manifold) of the rigid body to be the space (or manifold) where a point of which corresponds to a unique configuration of the rigid body. This space is denoted by M. Since three parameters are needed to specify an orientation and three more parameters are needed to specify a position, the configuration space (or configuration manifold) M has dimension six. As in [24], we will let the first three coordinates of M specify orientations of the body frame and the last three coordinates of M specify positions of the body frame. Let m $\in$ M be a nominal configuration of the rigid body and U_m be a neighborhood of m in M. We assume that at configuration m the body frame $x-y-z$ coincides with the inertial frame $X-Y-Z$. Then, there exists a natural coordination map

$$\psi: U_m \subset M \rightarrow R^6$$

given by

$$\psi(m) = (0, \cdots 0); \tag{2.1-1}$$

and

$$\psi(p) = (\theta_1, \theta_2, \theta_3, x_1, x_2, x_3), \quad \text{for all } p \in U_m$$

where θ_i's are the Euler angles and x_i's the coordinates of the body frame origin o at configuration p.

If g(t) is a C^1 curve in M representing the trajectory of a rigid body, then the generalized velocity of the rigid body is given by $\frac{d}{dt}g(t) \in T_{g(t)}M$, where $T_m M$ is the tangent space of M at configuration m ([17]). The trajectory of g(t) in local coordinates (namely, those given by (2.1-1)) can be written

$$\tilde{g}(t) = \psi \circ g(t) = (\theta_1(t), \theta_2(t), \theta_3(t), x_1(t), x_2(t), x_3(t))$$

Assume that $g(t_0) = m$, the generalized velocity at $(t = t_0)$ in local coordinates is given by (using the chain rule)

$$\frac{d}{dt}\tilde{g}(t) = \frac{\partial\psi}{\partial p}|_{g(t_0)}\frac{d}{dt}g(t)|_{t_0}$$

$$= (\omega_1,\omega_2,\omega_3,v_1,v_2,v_3) = (\omega,v) \quad (2.1\text{-}2)$$

where $\omega = (\omega_1, \omega_2, \omega_3)$ and $v = (v_1, v_2, v_3)$ are respectively the angular and the linear velocity of the rigid body relative to the axes of the inertial reference frame. In terms of the Euler angles $(\theta_1, \theta_2, \theta_3)$ the angular velocity ω can be expressed as

$$\omega_1 = \dot{\theta}_3 - \dot{\theta}_1\sin\theta_2$$

$$\omega_2 = \dot{\theta}_2\cos\theta_3 + \dot{\theta}_1\cos\theta_2\sin\theta_3$$

$$\omega_3 = \dot{\theta}_1\cos\theta_2\cos\theta_3 - \dot{\theta}_2\sin\theta_3$$

the linear velocity v is given by

$$v = (v_1, v_2, v_3) = (\dot{x}_1, \dot{x}_2, \dot{x}_3)$$

The linear map

$$\psi_*: T_m M \rightarrow R^6 \quad (2.1\text{-}3)$$

defined by

$$\psi_*(\xi) = \frac{\partial\psi}{\partial p}|_m \xi$$

is called the tangent map of ψ. The vector (ω, v) is also called the coordinate expression of a generalized velocity $\xi \in T_m M$.

Remark: (1). The coordination map ψ defined in (2.1-1) is only local. Unfortunately, there exists no global coordination map for the configuration manifold M and M does not support a natural positive definite metric. Consequently, the space $T_m M$ is geometrically different from R^6 [22].

Denote the set of generalized forces that can be exerted on the rigid body at configuration m by $T_m^* M$. It is also called the cotangent space of M at m and consists of all linear functionals defined on $T_m M$. An element $\eta \in T_m^* M$ is a combination of a linear force with a linear moment about the origin O in the inertial frame (Recall that both frames coincide at configuration m). The coordinate expression of $\eta \in T_m^* M$ is given by the dual linear map of (2.1-3) which is defined as follows [17].

$$\psi^{*}: R^{6} \rightarrow T_{m}^{*}M$$

and

$$<\xi, \eta> \equiv <\xi, \psi^{*}(\sigma)> = <\psi_{*}(\xi), \sigma> \qquad (2.1\text{-}4a)$$

where the pairing on the left of (2.1-4a) gives precisely the work done per unit time of a generalized force η on a generalized velocity ξ when viewed as a generalized displacement per unit time. The pairing on the right of (2.1-4a) is given by the inner product of two vectors in R^6

$$<\psi_{*}(\xi), \sigma> = <(\omega, \nu), (f, m)> = \omega^{t} m + \nu^{t} f \qquad (2.1\text{-}4b)$$

The vector $\sigma = (\psi^{*})^{-1}(\eta) = (f, m)$ is called the coordinate expression of a generalized force $\eta \in T_{m}^{*}M$, with the vectors $f = (f_1, f_2, f_3)$ and $m = (m_1, m_2, m_3)$ identified as the linear force and the angular moment about the inertial frame respectively applied to the rigid body. From now on we will write, for notational convenience, that a generalized velocity ξ as $\xi = (\omega, \nu) \in T_{m}M$ and a generalized force η as $\eta = (f, m) \in T_{m}^{*}M$. The work done per unit time of η with respect to ξ is given by (2.1-4b).

Remarks: (2). Let E(3) denote the Euclidean group of R^3, i.e. it consists of elements of the form (A, b), where A $\in$ SO(3), the space of 3 by 3 unitary matrices over the reals, and b $\in R^3$, with group multiplication defined by $(A_1, b_1)(A_2, b_2) = (A_1A_2, A_1b_2 + b_1)$. The identity element e of E(3) is (I, 0) with I being the 3 by 3 identity matrix. The group E(3) acts on R^3 according to

$$(A, b)x = Ax + b, \quad \text{for all } x \in R^3$$

and it is also referred to as the group of rigid motions in R^3. By identifying the nominal configuration m with the identity element e of E(3), and a given configuration p of M with the element of E(3) that translates the body from m to p, we obtain a natural isomorphism (given by (2.1-1)) between M and E(3) ([18]).

(3). The pairing in (2.1-4b) is induced by a hyperbolic metric on M. For the purpose of simplicity we will not distinquish the space T_m^*M from R^6 in the following studies although they are geometrically different (see remark (1)). The result we obtain however will still be valid when this distinction called for.

(4). In the literature ([11], [7], & [12]) a generalized velocity ξ is often called a twist, whereas a generalized force η a wrench.

If we use the standard basis $(e_1, \cdots e_6)$ for R^6, a wrench η applied to a rigid body can always be expressed as a linear combination of these basis wrenches (or screws) ([7], [11], [5]).

Suppose now that two rigid bodies A and B are in contact and assume that no energy is either stored or dissipated. We let $C^* \subset T_m^*M$ denote the set of contact wrenches that can be applied to B (by A) through the contact. The *Principle of Virtual Work* states that the set of allowable twists $\xi \in T_m M$ of rigid body B relative to rigid body A must satisfy

$$<\xi, \eta> = 0, \text{ for all } \eta \in C^* \tag{2.1-5}$$

where the inner product is defined in (2.1-4), in order to keep A and B in contact.

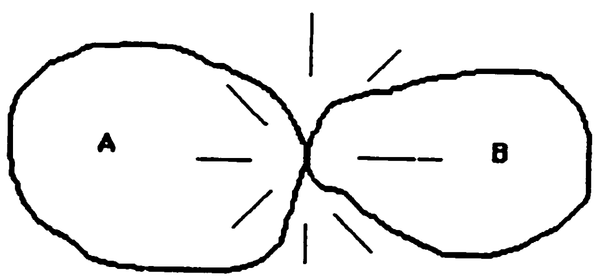

Figure 2. Two rigid bodies in contact

Contacts can always be thought of as constraints on the motion of a rigid body. For a given set $C^* \subset T_m^*M$, we define a set C $\subset T_m M$ by

$$C = \{ \xi \in T_m M, \text{ such that } <\xi, \eta> = 0, \text{ for all } \eta \in C^* \} \tag{2.1-6}$$

C is called the annihilator of C^* in $T_m M$. With these definitions, we state the Principle of Virtual Work as a theorem.

Theorem 2-1: When a rigid body B is constrained such that the set of contact wrenches can be exerted on B is $C^* \subset T_m^* M$, the set of allowable twist motions of B is precisely the annihilator C of C^* in $T_m M$.

2.2 Grasping Structures

We shall be concerned in this paper mainly with three basic contact types: (1). a point contact without friction, (2). a point contact with friction and (3) a soft finger contact. These contact types along with others are studied extensively in the literature ([5], [6], [7], & [9]). Define by n_c the number of independent contact wrenches that can be exerted on a rigid body at the contact. We have n_c equal to 1 for point contact without friction and 3 for point contact with friction. While for a soft finger contact n_c equals to 4, and for more general contacts such as contact of a line with a plane, etc. the value of n_c may be found in Table 2-3 of [5]

Before we give a formal definition of a contact, let us look at the following example, which we will use repeatedly in the paper.

Example 2-2: Consider a three fingered robot hand contacting a cube as shown. Assume that finger I can be modeled as a point contact without friction, finger II as a point contact with friction, and finger III as a soft finger contact. With the body coordinate x-y-z as shown in the figure, let us obtain a matrix representation of each contact map represented as maps from the applied independent contact forces to the wrench space of the object as follows.

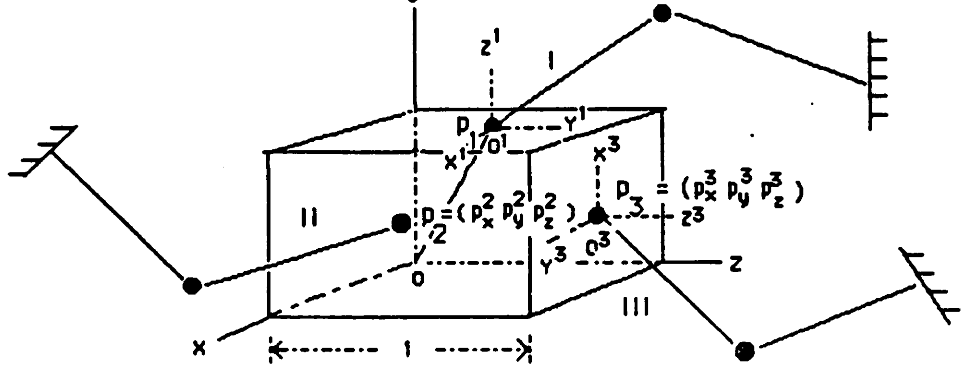

Figure 3. Three fingered hand contacting a cube

Finger *I*: ψ_{c1} is a map taking the normal finger force applied at finger I to the body wrenches (Torques are measured relative to o).

$$\psi_{c1}: R^1 \rightarrow T_m^* M \tag{2.2-1a}$$

$$\psi_{c1}(x) = \begin{bmatrix} f_1^1 \\ f_1^1 \times (p_1 - o) \end{bmatrix} x = \begin{bmatrix} 0 \\ 0 \\ 1 \\ -p_y^1 \\ p_x^1 \\ 0 \end{bmatrix} [x]$$

Finger *II*: ψ_{c2} is a map taking the three applied finger forces at finger II: namely the normal force and two orthogonal friction forces into the body wrench.

$$\psi_{c2}: R^3 \rightarrow T_m^* M \tag{2.2-1b}$$

$$\psi_{c2}(x_1, x_2, x_3) = \begin{bmatrix} f_1^2 & f_2^2 & f_3^2 \\ f_1^2 \times (p_2 - o) & f_2^2 \times (p_2 - o) & f_3^2 \times (p_2 - o) \end{bmatrix} \begin{bmatrix} x_1 \\ x_2 \\ x_3 \end{bmatrix}$$

$$= \begin{bmatrix} 1 & 0 & 0 \\ 0 & 1 & 0 \\ 0 & 0 & 1 \\ 0 & p_z^2 & -p_y^2 \\ -p_z^2 & 0 & p_x^2 \\ p_x^2 & -p_x^2 & 0 \end{bmatrix} \begin{bmatrix} x_1 \\ x_2 \\ x_3 \end{bmatrix}$$

Finger *III*: ψ_{c3} is a map taking the three finger forces and one normal torque applied at finger III into the body wrench.

$$\psi_{c3}: R^4 \rightarrow T_m^* M \tag{2.2-1c}$$

$$\psi_{c3}(x_1,x_2,x_3,x_4) = \begin{bmatrix} f_1^3 & f_2^3 & f_3^3 & 0 \\ f_1^3 \times (p_3 - o) & f_2^3 \times (p_3 - o) & f_3^3 \times (p_3 - o) & m_4^3 \end{bmatrix} \begin{bmatrix} x_1 \\ x_2 \\ x_3 \\ x_4 \end{bmatrix}$$

$$= \begin{bmatrix} 0 & 1 & 0 & 0 \\ 1 & 0 & 0 & 0 \\ 0 & 0 & 1 & 0 \\ p_z^3 & 0 & -p_y^3 & 0 \\ 0 & -p_z^3 & p_x^3 & 1 \\ -p_x^3 & p_x^3 & 0 & 0 \end{bmatrix} \begin{bmatrix} x_1 \\ x_2 \\ x_3 \\ x_4 \end{bmatrix}$$

Notice that f_1^i and m_4^i in the above equations are the unit normals to the contact surface (i.e., surfaces of the rigid body) at the *ith* contact point. f_2^i and f_3^i are the unit tangent vectors to the contact surface and they determine along with f_1^i an orthonormal basis at the *ith* contact point.

Motivated by this and similar examples, we define a contact as following:

Definition 2-3: *(of contact) A contact upon a rigid body at configuration m is a map*

$$\psi_c : R^{n_c} \rightarrow T_m^* M \qquad (2.2\text{-}2)$$

for some n_c defined as the number of independent contact wrenches that can be exerted on the rigid body at the contact and depends on the structure of the contact only.

Similarly, we define a grasp of a rigid body by a robot hand as a group of contacts. For this we assume the hand has k fingers, each finger contacts the object at one point (at the fingertip only) and defines a contact map $\psi_{ci} : R^{n_i} \rightarrow T_m^* M$, for i = {1, ... k}.

Definition 2-4: *A grasp of a rigid body at configuration m by a robot hand with k fingers is a map*

$$G : R^n \rightarrow T_m^* M, \; n = \sum_{i=1}^{i=k} n_i,$$

given by

$$G(x_1, x_2, \cdots x_n) = \sum_{i=1}^{i=k} \psi_{ci}(x_{n_{i-1}+1}, \cdots x_{n_i}) \tag{2.2-3}$$

Remark (5): Given a grasping configuration, we outline here a procedure to obtain a matrix representation of the grasp map: (1). specify a body coordinate and obtain the coordinates of each contacting point. (2). determine the unit normal and the two orthonormal tangent vectors to the contacting surface at the contact point.(3). pick a torque origin in the body coordinate and construct for each contact map the contact matrix as in Example 2-2, and (4). concatenate these contact matrices side by side into a big matrix, this is our grasp matrix for the particular choice of body coordinate and particular choice of torque origin.

For example, the grasp map of Figure 3 is obtained by adding the contact maps (2.2-1a, b & c), i.e.,

$$G = \left[\begin{matrix} f_1^1 & f_1^2 & f_2^2 & f_3^2 \\ f_1^1 \times (p_1 - 0) & f_1^2 \times (p_2 - o) & f_2^2 \times (p_2 - o) & f_3^2 \times (p_2 - o) \end{matrix} \right.$$

$$\left. \begin{matrix} f_1^3 & f_2^3 & f_3^3 & 0 \\ f_1^3 \times (p_3 - o) & f_2^3 \times (p_3 - o) & f_3^3 \times (p_3 - o) & m_4 \end{matrix} \right]$$

$$= \begin{bmatrix} 0 & 1 & 0 & 0 & 0 & 1 & 0 & 0 \\ 0 & 0 & 1 & 0 & 1 & 0 & 0 & 0 \\ 1 & 0 & 0 & 1 & 0 & 0 & 1 & 0 \\ -p_y^1 & 0 & p_z^2 & -p_y^2 & p_z^3 & 0 & -p_y^3 & 0 \\ p_x^1 & -p_z^2 & 0 & p_x^2 & 0 & -p_z^3 & p_x^3 & 1 \\ 0 & p_x^2 & -p_x^2 & 0 & -p_x^3 & p_x^3 & 0 & 0 \end{bmatrix} \tag{2.2-4}$$

2.3 Wrench Transformation Matrices

In obtaining a matrix representation of a grasp map, it is often convenient to first get the finger contact wrenches relative to coordinate systems at the contacting points and then transform these contacting wrenches to the body coordinate. This is done using a wrench transformation matrix (Kerr [7]) and we discuss a procedure of obtaining such a matrix with example 2-2. The idea of using wrench transformation matrices will become clear after the following example.

As shown in Figure 3, we attach finger coordinate system $x^i - y^i - z^i$ at each contact point, where the z^i axis is always normal to the contact surface (assuming the rigid body have well defined normals almost everywhere). Let the coordinate system $x^i-y^i-z^i$ be related to the body coordinate x-y-z by $(A_i, p_i) \in E(3)$, where $A_i \in SO(3)$ is the orientation of $x^i-y^i-z^i$ relative to x-y-z and p_i is the translation of the origin o^i. A point $\tilde{q}$ in $x^i-y^i-z^i$ is transformed to a point q in x-y-z according to

$$q = A_i\tilde{q} + p_i \tag{2.3-1}$$

In the body coordinate let $p_i - o = (p_x^i, p_y^i, p_z^i)$ and define the cross product operator constructed from $(p_i - o)$ by

$$S(p_i - o) = \begin{bmatrix} 0 & -p_z^i & p_y^i \\ p_z^i & 0 & -p_x^i \\ -p_y^i & p_x^i & 0 \end{bmatrix} \tag{2.3-2}$$

It is easy to see that $S(p_i - o)f = (p_i - o)\times f$ for any $f \in R^3$. Any linear force $\tilde{f}_i$ in the *ith* finger coordinate is transformed to a linear force f_i in the body coordinate as follows

$$f_i = A_i\tilde{f}_i \tag{2.3-3a}$$

and the corresponding torque about "o" is

$$f_i \times (p_i - o) = S(o - p_i)A_i\tilde{f}_i \tag{2.3-3b}$$

More generally, a contact wrench $\tilde{e}_i$ in the finger coordinate is transformed to a contact wrench e_i in the body coordinate by

$$e_i = \begin{bmatrix} A_i & 0 \\ S(o - p_i)A_i & A_i \end{bmatrix} \tilde{e}_i = T_{f_i}\tilde{e}_i \tag{2.3-4}$$

Note that (2.3-3a & b) are special cases of (2.3-4) with $\tilde{e}_i$ being only a linear force. The matrix T_{f_i} is called the wrench transformation matrix of finger i, it transforms contact wrenches at the *ith* finger coordinate to contact wrenches in the body coordinate. On the other hand, any contact wrench $\tilde{e}_i$ in the *ith* finger coordinate can be expressed as a linear combination of the basis wrenches $(e_1^i, \cdots e_{n_i}^i)$ determined by the contact types of the ith contact, i.e.,

$$\tilde{e}_i = \begin{bmatrix} e_1^i , e_2^i , \cdots e_{n_i}^i \end{bmatrix} \begin{bmatrix} x_1 \\ x_2 \\ \cdot \\ \cdot \\ \cdot \\ x_{n_i} \end{bmatrix} = B_i \begin{bmatrix} x_1 \\ x_2 \\ \cdot \\ \cdot \\ \cdot \\ x_{n_i} \end{bmatrix} \tag{2.3-5}$$

The matrix B_i is called the ith constraint matrix and contains ith contact constraint information.

Consequently, the wrench transformation matrix T_f and the constraint matrix B of the hand in Figure 3 are formed from these T_{f_i} and B_i as

$$T_f = \begin{bmatrix} A_1 & 0 & A_2 & 0 & A_3 & 0 \\ S(o-p_1)A_1 & A_1 & S(o-p_2)A_2 & A_2 & S(o-p_3)A_3 & A_3 \end{bmatrix} \tag{2.3-6}$$

and

$$B = \begin{bmatrix} B_1 & B_2 & B_3 \end{bmatrix} = \begin{bmatrix} 0 & | & 0 & 0 & 1 & | & 0 & 0 & 1 & 0 \\ 0 & . & 0 & 1 & 0 & . & 0 & 1 & 0 & 0 \\ 1 & | & 1 & 0 & 0 & | & 1 & 0 & 0 & 0 \\ 0 & . & 0 & 0 & 0 & . & 0 & 0 & 0 & 0 \\ 0 & | & 0 & 0 & 0 & | & 0 & 0 & 0 & 0 \\ 0 & . & 0 & 0 & 0 & . & 0 & 0 & 0 & 1 \end{bmatrix} \tag{2.3-7}$$

Direct computation shows that the grasp matrix G of (2.2-4) is the product of the wrench transformation matrix T_f and the constraint matrix B, i.e., G = T_f B.

Thus, we see that a grasp matrix G can always be factored as a product of two matrices T_f and B (Kerr [7]). The wrench transformation matrix T_f transforms contact wrenches from finger coordinates into the body coordinate. It contains contact configuration information, while the constraint matrix B contains contact constraint information. While varying contact types only B changes, when contact configuration vary T_f alone changes.

2.4 Grasping under Unisense and Finite Frictional Forces

In definition (2-3) (or (2-4)) we have implicitly assumed bi-directional and infinite frictional forces by allowing the force domain of the contact map (or the grasp map) to range over the entire space R^{n_c} (or R^n). But, this does not happen in reality when two objects in contact can not pull on each other (without glue or field force attraction) and sliding phenomena are frequently observed even between very rough contacting surfaces. To handle unisense and finite frictional forces, we will need to restrict the (force) domain of a contact map (or grasp map) to an appropriate subset of R^{n_c} (or R^n). Consider again the example of Figure 3, assuming Coulomb frictional models for each contact, we obtain force domain of the contact map ψ_{ci}:

$$\psi_{c1}\text{: } K_1 = \{x \in R^1, \text{ such that } x \geqslant 0\}$$

$$\psi_{c2}\text{: } K_2 = \{x \in R^3, \text{ such that } x_1 \geqslant 0, x_2^2 + x_3^2 \leqslant \mu_1^2 x_1^2\} \qquad (2.4\text{-}1)$$

$$\psi_{c2}\text{: } K_3 = \{x \in R^4 \text{ such that } x_1 \geqslant 0, x_2^2 + x_3^2 \leqslant \mu_2^2 x_1^2, |x_4| \leqslant \mu_t x_1\}$$

where μ_i's are the Coulomb friction coefficients of the respective contacting surface pairs, and μ_t the torsional friction coefficient ([7]). In [9] a different model of the soft finger contact is used giving a different set K_3 in R^4. The force domain K of a grasp map (2.2-4) is thus the product of each contact force domain K_1, K_2 and K_3 in the product space $R^1 \oplus R^3 \oplus R^4 = R^8$.

The force domain of a contact map modeled by Coulomb frictional law has a very nice property: convexity.

Proposition 2-5: The set K_i for i = {1, ... 3} in (2.4-1) is a convex cone.

Proof.

It suffices to show that K_3 is a convex cone. Let x and $y \in K_3$. Then for $\alpha \geqslant 0$ we have

$$\alpha x = (\alpha x_1, \alpha x_2, \alpha x_3, \alpha x_4)$$

obviously, $\alpha x_1 \geqslant 0$ and,

$$(\alpha x_2)^2 + (\alpha x_3)^2 = \alpha^2(x_2^2 + x_3^2) \leqslant \mu^2(\alpha x_1)^2.$$

also $|\alpha x_4| = \alpha |x_4| \leqslant \mu_t(\alpha x_1)$. Therefore, $\alpha x \in K_3$.

Let $\qquad x_2 = \mu x_1 \cos\theta_1, \; x_3 = \mu x_1 \sin\theta_1$

and $y_2 = \mu y_1 \cos\theta_2,\ y_3 = \mu y_1 \sin\theta_2$

then

$$(x_2+y_2)^2 + (x_3+y_3)^2 = \mu^2(x_1^2 + y_1^2 + 2x_1 y_1 \cos(\theta_2 - \theta_1))$$

$$\leqslant \mu^2(x_1+y_1)^2$$

and $$|x_4+y_4| \leqslant |x_4| + |y_4| \leqslant \mu_t(x_1+y_1)$$

thus, $(x+y) \in K_3$. Q.E.D.

Corollary 2-6: The product of convex cones is again a convex cone in the product space. Consequently the force domain K of the grasp map (2.2-4) is a convex cone.

2.5 Stability of a Grasp and Body Coordinate Transformations

In robot hand applications, we are interested in characterizing the stability of a grasp. We say that a grasp is *stable* (or *statically stable*) if and only if it can balance disturbance forces in all directions.

Proposition 2-7: A grasp G defined in (2.2-3) is statically stable if and only if the associated grasp map is surjective.

Proof.

Suppose that G is surjective, then for any disturbance wrench $\omega_d \in T_m^* M$, there exists a finger force $x \in R^n$ such that

$$G(x) = \omega_d \tag{2.5-1}$$

i.e., the disturbance wrench is exactly balanced out by the contact wrench. The converse part follows from the definition. Q.E.D.

Corollary 2-8: A grasp G with associated force domain K $\subset R^n$ is (statically) stable if and only the associated grasp map G restricted to K is surjective.

In the following discussion, the set K $\subset R^n$ always refers to the force domain of a grasp map G. It is a convex cone in R^n and may be the entire space. When the set K equals to R^n, the stability condition for a grasp G requires that the grasp matrix be full row rank. For a proper subset K of R^n, we define

$$B_1^n = \{x \in R^n, \| x \|_2^2 \leqslant 1\} \tag{2.5-2}$$

to be the unit ball of R^n and let O_ϵ denotes an ϵ open ball at the origin of R^6 (= T_m^*M). With these notations, we have

Proposition 2-9: A grasp G with force domain K is stable if and only if there exists an $\epsilon > 0$, such that

$$O_\epsilon \subset G(K \cap B_1^n). \tag{2.5-3}$$

Proof.

Suppose (2.5-3) is true, then for any $y \in T_m^*M$, there exists $\alpha > 0$, such that $\frac{\|y\|}{\alpha} \leqslant \epsilon$. Let $\tilde{y} = \frac{y}{\alpha}$, then $\tilde{y} \in O_\epsilon$ and (2.5-3) implies existence of $\tilde{x} \in (K \cap B_1^n)$ such that

$$G(\tilde{x}) = \tilde{y} = \frac{y}{\alpha}$$

$$\rightarrow G(\alpha\tilde{x}) = y$$

But the set K is a convex cone, therefore $x = \alpha\tilde{x} \in$ K, and $G|_K$ is surjective. Q.E.D.

Proposition (2-9) alleviates the burden of checking the stability of a grasp with a restricted force domain. Modified algorithms of [15] can be used to perform the test (2.5-3) and further details on this issue are discussed in Section 3.4.

From previous examples, we see that the matrix representation of a grasp map depends not only on finger contacting locations but also on the choice of the body coordinate system. For fixed contacting locations and fixed contacting structures we may obtain different grasp matrices as we vary the body coordinate system, assuming torque origin of the grasp matrix coincides with the origin of each body coordinate system. From Remark (2), any change of body coordinate system may be described by an element of E(3) - the Euclidean group of R^3. Thus, let $T \in E(3)$ represents a body coordinate change from $x-y-z$ to an new body coordinate $x'-y'-z'$. Then a point x in the old body coordinate system is transformed to a point $\tilde{x}$ in the new body coordinate system according to

$$\tilde{x} = T(x) = Ax + b \tag{2.5-4}$$

where A ∈ SO(3), and $b \in R^3$. Suppose that the matrix representation of a contact map with respect to x-y-z is given in (2.2-1c), then it is easy to verify that under body coordinate change by T the matrix representation of the contact map is transformed to

$$\tilde{\psi}_{c3} = \begin{bmatrix} Af_1^3 & Af_2^3 & Af_3^3 & 0 \\ Af_1^3 \times A(p_3 - o) & Af_2^3 \times A(p_3 - o) & Af_3^3 \times A(p_3 - o) & Am_4^3 \end{bmatrix}$$

$$= \begin{bmatrix} A & 0 \\ 0 & A \end{bmatrix} \begin{bmatrix} f_1^3 & f_2^3 & f_3^3 & 0 \\ f_1^3 \times (p_3 - o) & f_2^3 \times (p_3 - o) & f_3^3 \times (p_3 - o) & m_4^3 \end{bmatrix}$$

$$= \tilde{T} \psi_{c3} \tag{2.5-5}$$

where $\tilde{T}$ is the diagonal matrix with A's on the diagonal. Hence, it follows that the matrix representation of any grasp map under body coordinate transformation by T can be expressed as

$$\tilde{G} = \tilde{T} G \tag{2.5-6}$$

We may also obtain, for fixed grasping locations and a fixed body coordinate system, different grasping matrices by changing the torque origin o to a new point b about which the grasp matrix is constructed. To get the new matrix, let $(b - o) = (b_1, b_2, b_3)$ and define A to be the skew symmetric matrix constructed from $(b - o)$ according to (2.3-2), i.e.,

$$A = \begin{bmatrix} 0 & -b_3 & b_2 \\ b_3 & 0 & -b_1 \\ -b_2 & b_1 & 0 \end{bmatrix}$$

we have for any $f \in R^3$,

$$Af = (b - o) \times f = f \times (o - b) \tag{2.5-7}$$

and

$$\tilde{G} = \begin{bmatrix} f_1^1 & f_2^1 & \cdots & 0 \\ f_1^1 \times (p_1 - b) & f_2 \times (p_1 - b) & \cdots & m_4^k \end{bmatrix}$$

$$= \begin{bmatrix} f_1^1 & f_2^1 & \cdots & 0 \\ f_1^1 \times (p_1 - o) + f_1^1 \times (o - b) & f_2^1 \times (p_1 - o) + f_2^1 \times (o - b) & \cdots & m_4^k \end{bmatrix}$$

$$= \begin{bmatrix} I & 0 \\ A & I \end{bmatrix} \begin{bmatrix} f_1^1 & f_2^1 & \cdots & 0 \\ f_1^1 \times (p_1 - o) & f_2^1 \times (p_1 - o) & \cdots & m_4^k \end{bmatrix} \tag{2.5-8}$$

$$= \hat{T}_b G$$

i.e., change of torque origin corresponds to multiply the original grasp matrix on the left by a nonsingular matrix $\hat{T}_b$.

Remark: (6) $\tilde{T}$ is unitary, i.e., $\tilde{T}^t \tilde{T} = I$ while $\hat{T}_b$ is not. This is important since unitary matrices preserve norm.

Theorem 2-10: Stability properties of a grasp map G are invariant under body coordinate transformation and under change of torque origin.

Proof.

From (2.5-6) or (2.5-8), $\tilde{T}$ or $\hat{T}_b$ is nonsingular and surjectivity of G is thus preserved. Q.E.D.

Example 2-11: Consider again the grasp of Figure 3, whose matrix representation is given in (2.2-4). Using a modification of the algorithms of [15] it may be shown that, with all friction coefficients set to 1, G(K $\cap B_1^n$) contains an open ball at the origin of radius 0.2. Therefore, the grasp G by Proposition (2-9) is stable.

3. Optimal Grasping Theory

We have studied static stability of a grasp, and defined a stable grasp in terms of its ability to reject disturbance forces. A deeper question to ask ourselves now is: Which grasp should one choose when given a set of *stable* grasps ? To answer this question we introduce the concept of optimal grasping. We will propose several alternative "grasp quality" measures which can be used to evaluate a grasp.

The idea of optimal grasping was inspired by a study of linear control theory, where the term controllability grammian is often used to characterize the quality of a system's controllability. In grasping theory we say that a grasp G_1 is "better" ($\geqslant$) than a grasp G_2 if G_1 achieves a better figure of merit in terms of a certain quality measure.

3.1 Quality Measure δ: Smallest Singular Value of G

Consider a grasp G defined in (2.2-3). We define the quality $\delta(G)$ of a grasp G as

$$\delta(G) = \sigma_{min}(G) \tag{3.1-1a}$$

where $\sigma_{\min}(G)$ stands for the smallest singular value of the matrix G. We say that $G_1 \geqslant G_2$ if and only if $\delta(G_1) \geqslant \delta(G_2)$.

(3.1-1a) gives a worst case analysis of a grasp. It should be noticed that a grasp G is stable if and only $\delta(G) > 0$. Hence, the quality measure $\delta(.)$ captures the stability property of a grasp. Using the quality measure (3.1-1a), we could then answer the question posed before, namely we would chose among a set of stable grasps one which maximizes its minimum singular value. This grasp is called the "optimal grasp" with respect to the quality measure (3.1-1a). Technical details of finding such an optimal grasp for a rigid body are provided in Section 3.5.

In (3.1-1a), we have implicitly assumed the set K to be the entire space R^n. For a general set K, we modify (3.1-1a) to

$$\delta(G) = \underset{y \in R^n}{Inf} \{ \| y \| \text{ such that } y \notin G(B_1^n \cap K) \} \tag{3.1-1b}$$

i.e., the measure $\delta(G)$ is the minimum distance of the complement of the set $G(B_1^n \cap K)$ to the origin of R^6. (3.1-1b) would give the smallest singular value of G when the set K is R^n itself. We notice from remark (6) that, while the measure $\delta(.)$ in (3.1-1a) and (3.1-1b) is invariant under body coordinate transformations it is *not invariant* under change of torque origin. Thus, one should be very careful in selecting the torque origin of the grasp matrix in using this quality measure.

3.2 Quality Measure ν: Volume in Wrench Space

While the quality measure (3.1-1) has the obvious advantage of geometric and computational simplicity, it is not invariant under change of torque origin. Also, since it gives only a worst case analysis it does not reflect uniformity of the grasp. To avoid these problems we introduce a quality measure which is invariant under both change of body coordinate and change of torque origin. We call such a measure a bi-invariant volume measure (see Theorem 3-2). The volume measure $\nu(G)$ of a grasp G is defined as

$$\nu(G) = \int_{G(B_1^n \cap K)} dv \tag{3.2-1}$$

i.e., it is the volume in T_m^*M of the set $G(B_1^n \cap K)$. When the set K constitutes the entire space R^n, computation of (3.2-1) is especially simple, as given by

Proposition 3-1: Let σ_1, σ_2, ... σ_6 denote the set of singular values of a grasp matrix G. Then there exists a $\beta > 0$ such that for the case K = R^n,

$$\nu(G) = \beta(\sigma_1 \sigma_2 \cdots \sigma_6) \tag{3.2-2}$$

Proof.

it follows from the definition of singular values of a matrix. Q.E.D.

The volume measure $\nu(.)$ is uniform in all directions. Furthermore, it is bi-invariant, i.e., we have

Theorem 3-2: The volume measure $\nu(.)$ of (3.2-1) is invariant under both body coordinate transformation and change of torque origin.

Proof.

The proof for the general case of (3.2-1) follows from the Change of Variable Theorem in integration theory, see Boothby [17]. We give a direct proof in the special case K = R^n. Let T $\in$ E(3) be a body coordinate transformation. We know from (2.5-6) that the transformed matrix representation $\tilde{G}$ is related to G by $\tilde{G} = \tilde{T}G$. By (3.2-2) there exists $\beta > 0$ such that

$$\nu(\tilde{G}) = \beta\{\det(\tilde{G}\ \tilde{G}^t)\}^{1/2} = \beta\{\det(\tilde{T}\ G\ G^t\ \tilde{T}^t)\}^{1/2}$$

$$= \beta\{\det(\tilde{T})\ \det(G\ G^t)\ \det(\tilde{T}^t)\}^{1/2} = \beta\{\det(A)^2\ \det(G\ G^t)\ \det(A)^2\}^{1/2}$$

$$= \beta\ \{\det(GG^t)\}^{1/2} = \nu(G)$$

since $A \in SO(3)$ its determinant is 1. The proof for change of torque origin follows similarly. Q.E.D.

Remark: (7). For a bi-invariant quality measure such as $\nu(.)$, we can first construct the grasp matrix with respect to any coordinate frame and any torque origin and then perform the evaluation. The result we would obtain by doing so is not altered if we evaluate another grasp map with respect to a different coordinate frame and a different torque origin.

One problem associated with volume measure (3.2-1) is that it does not reflect the stability properties of a grasp G when the set K is a proper subset of R^n. The image set of $(B_1^n \cap K)$ may be a half space in $T_m^* M$ but have nonzero volume measure. Therefore, to compare the qualities of two given grasps, we have to first check the stability requirement and then use (3.2-1). Section 3.4 presents numerical considerations regarding computation of $\nu(.)$ under its general case.

Example 3-3: Consider the following two grasps of a three fingered hand of a hexagon, with all finger contacts modeled as point contacts with friction and all friction coefficients set to 1.

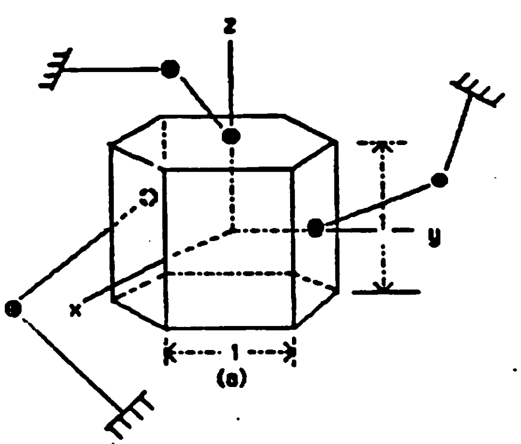

(a)

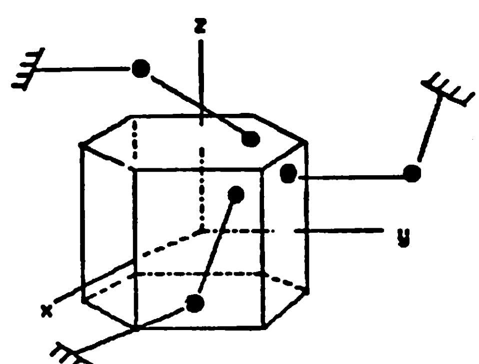

(b)

Figure 4. Two set of different grasp configurations to an hexagon.

The geometry of the hexagon and details of each grasping configuration are shown in the figure. Along the line of discussions from the previous chapter, we constructed grasp matrices G_1 and G_2 (with "o" being the torque origin) for grasp configuration (a) and (b). The force domain of each grasp map is defined from given assumptions, and the quality measures $\delta(.)$ & $\nu(.)$ of G_1 & G_2 are computed as (see Section 3.4):

$$\delta(G_1) = 0.768, \quad \delta(G_2) = 0.357$$

$$\nu(G_1) = 26.7 \quad \nu(G_2) = 7.85$$

Hence, grasp (a) is better than grasp (b); and this is consistent with practical experience as the reader can readily verify.

3.3 Task Oriented Quality Measure μ

We have introduced two quality measures that can be used to evaluate a grasp. These quality measures all reflect one key concept, namely the " absolute degree" of stability. In many applications, it suffices to find a grasp which is optimal with respect to these quality measures, i.e. (3.1-1) and (3.2-1). Typical examples in this category include pick-and-place operations under *uncertain environment* and disposing waste in a container. Tasks involved in this category are usually simple and knowledge of working environment is either not available or of less concern. However, in cases such as handling a tea cup, grasping a pencil and writing, and manipulating a workpiece in a *known environment*, it appears that the characterizations of (3.1-1) or (3.2-1) are not adequate. Consider the example of grasping a tea cup for the task of drinking. Obviously a human would not grasp the tea cup with his full hand encompassing the cup, even though it achieves a high quality measure by (3.1-1) or (3.2-1). Instead, she grasps the tea cup at the handle to achieve better manipulability, and in the pencil example she grasps near either end of a pencil to achieve better dexterity - a necessary requirement in writing. There are also other examples in our daily lives where a grasp is dictated more by task requirement than by a neat stability requirement. Humans use as much information about the task and the working environment as possible in determining the grasp, forces irrelevant to the task are weighted less than forces which are closely associated with the task. Also, under a known working environment a grasp is chosen according to the probability of occurrence of disturbances. In other words, we speak of task requirement - with stability requirement as a subset - in evaluating a grasp. A task oriented quality measure is then the basic ingredient in the study of optimal grasping theory. The questions to be answered then are: (1). how does one model a task and the robot working environment? and (2). how does one incorporate the model into a quality measure?

The first question has been widely addressed in the literature ([10]) but a clear and analytic solution is not provided. Consequently, we present an approach to modeling a task and the robot's working environment by an ellipsoid in the space T_m^*M. We call such an ellipsoid the ***task ellipsoid***. We will show that modeling the task and working environment by an ellipsoid is very natural and consistent with our grasping experience. We can, of course, in a more general setting ***model tasks by arbitrary convex sets*** in T_m^*M (an ellipsoid is a special convex set) but the approach is completely similar. Hence, we will restrict ourselves to modeling tasks by ellipsoids. An example with tasks modeled by an arbitrary convex set will however be given at the end of the section.

3.3.1 Task Ellipsoids

The following examples illustrate the procedure of modeling tasks and working environment by task ellipsoids.

Example 3-4: Consider the peg insertion problem depicted in Figure 5. The task requirement amounts to grasping the workpiece and inserting it into the hole.

In order to execute the task, a nominal trajectory is planned before the grasping action. The working environment (description of the hole) and geometry of the workpiece is assumed known. Suppose that the workpiece is grasped at some grasp configuration and the hand follows the planned trajectory until some misalignment of the peg or the hole causes the hand to deviate from the nominal trajectory and the workpiece or the hand to collide with the environment.

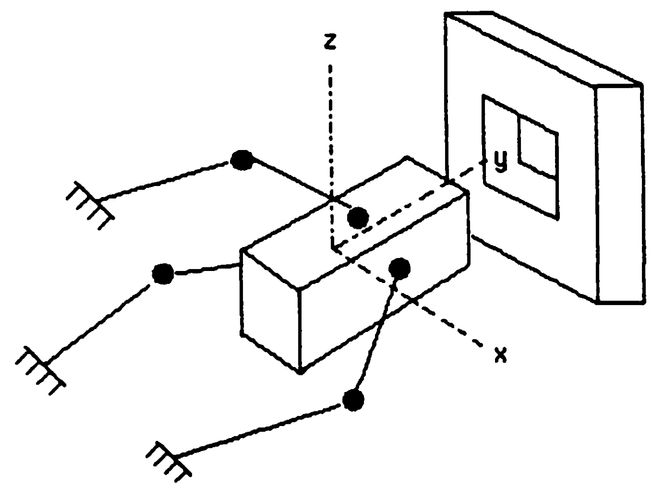

Figure 5. Peg-in-Hole Task

Choosing the body coordinate frame as shown, a study of the environment reveals that the likehood of collision in each force direction in the decreasing order should be $-f_y$, $\pm\tau_z$, $\pm\tau_x$, $\pm f_z$, $\pm f_x$, $\pm\tau_y$, $+f_y$. Let f_y also denote the magnitude of collision force in that direction and so on for other force components. To model this task, we look at a set A_β in the wrench space T_m^*M, parameterized by β, coefficients r_i, i = 1, .. 6 and constants c_i , i = 1, 2, as

$$A_\beta=\left\{(f_x ....\tau_z)\in R^6,\ \frac{(f_y+c_1)^2}{r_1^2}+\frac{\tau_z^2}{r_2^2}+\frac{\tau_x^2}{r_3^2}+\frac{(f_z-c_2)^2}{r_4^2}+\frac{f_x^2}{r_5^2}+\frac{\tau_y^2}{r_6^2}\leqslant\beta^2\right\} \qquad (3.3\text{-}1)$$

The set A_β is an ellipsoid in T_m^*M centered at $(0, -c_1, c_2, 0, 0, 0)$ with principal axis length given by $(r_i/\beta$, i=1, ..6). The shape of the ellipsoid is determined by the ratio of coefficient $(r_i)_{i=1}^{i=6}$ and location of the ellipsoid is given by the constants $(c_i)_{i=1}^{i=2}$. Therefore, varying the coefficients (r_i , i = 1, .. 6) and the constants (c_i , i = 1, 2), one can obtain various ellipsoids in the wrench space. The parameter β rescales the ellipsoid and in reality it corresponds to a choice of force unit.

By appropriately assigning a set of ratios to the coefficients (r_i, i =1 ... 6) and values to the constants (c_i i = 1,2) we can in principle use the ellipsoid A_β to represent the task force requirement of the peg-insertion task. It is apparent from the figure that the task requirement amounts to have $(r_i \geqslant r_j)$ if $(j \geqslant i)$. The constants c_1 reflects the offset of collisions in $+f_y$ and $-f_y$ directions. When it is unlikely to have collisions in $+f_y$ direction c_1 is set to a very large value. The constant c_2 reflects gravitational force on the workpiece. How to arrive at an exact set of values for r_i, i = 1, .. 6 (parameterized by β) and constants c_i , i = 1, 2, that meet the peg-insertion task requirement depends heavily on one's experiences with task modeling.

Example 3-5: Consider the problem of grasping a pencil for the task of writing. Our experience tells us that, in order to execute the task (writing), the grasping configuration should, (1). provide as much dexterity in the lead as possible and, (2). provide sufficient normal forces at the pencil lead. With the pencil configuration shown in Figure 6, the task specifications are translated into, (1). high torque requirement in $\pm\tau_z$ and $\pm\tau_y$ directions, (2). large normal force in $+f_x$ direction. If we could somehow obtain a set of ratios $(r_i)_{i=1}^{i=6}$ between the disturbance forces required by the task,

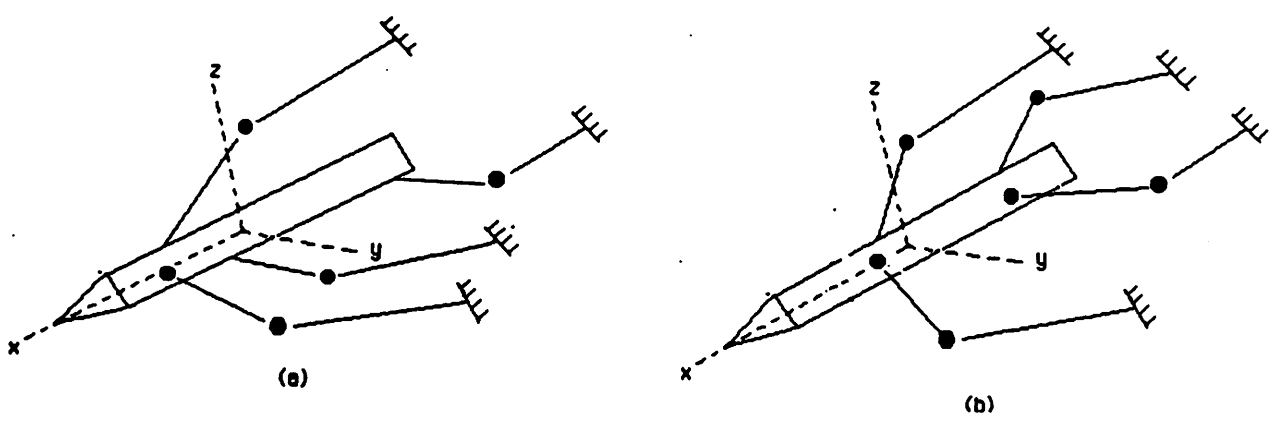

Figure 6. Two grasping configurations to a pencil

we get a task ellipsoid

$$A_\beta = \left\{ (f_x, \cdots \tau_z) \in R^6, \ \frac{\tau_z^2}{r_1^2} + \frac{\tau_2^2}{r_2^2} + \frac{(f_x - c)^2}{r_3^2} + \frac{f_y^2}{r_4^2} + \frac{f_z^2}{r_5^2} + \frac{\tau_x^2}{r_6^2} \leqslant \beta^2 \right\}. \quad (3.3\text{-}2)$$

parameterized by β, and the constant c representing the offset of the required task force in $+f_x$ direction with respect to $-f_x$ direction.

In pencil grasping, the process of accurately modeling the task requirement by an ellipsoid, i.e., finding the constants r_i and c in (3.3-2) that best describe the task, is quite complicated. Observe the human action in learning pencil grasping: initially, a child (with no previous experience) would probably grasp a pencil as shown in Figure 6 (b), to provide strong stability. But, such a grasp does not provide much dexterity at the pencil lead. So as the child grows up he learns from his experience or is taught by adults to modify his task ellipsoid and eventually grasp the pencil at the right configuration (a). This process is also manifested by the process of an adult in performing a unfamiliar task. After a few errors and trials, he could grasp the target object in the proper configuration so as to execute the task efficiently. It does take a great deal of modeling effort to specify a task ellipsoid for a specific task. Nevertheless, the difficulties can be reduced significantly because we could store our "experience" in computers and do task modeling once and for all.

Another example is the task of parts assembly, where a robot grasps a part and maneuvers it through a prescribed path in a cluttered environment. Suppose we can predict disturbance forces from the environment by some probability ratios, then with a fixed coordinate system, we can model the disturbance forces by an ellipsoid in T_m^*M. The direction of the disturbance forces correspond to the principal axes of the ellipsoid and lengths of principal axes are given by the probability ratios. Such a disturbance ellipsoid is also called a task ellipsoid for notational convenience. The grasp should then reject disturbance forces according to the ellipsoid.

Inspired by these examples, we will assume that our task is modeled by an ellipsoid given as in (3.3-3) below with Q a 6×6 positive definite symmetric matrix, and $a \in R^6$ reflecting the asymmetry in the task. Our goal then is to construct a quality measure that optimizes the grasp with respect to (3.3-3).

$$A_\beta = \{ y \in R^6 , <y, Qy> + <a, y> \leqslant \beta^2 \} \tag{3.3-3}$$

3.3.2 Task Oriented Quality Measure μ

Given a task (3.3-3), we now introduce a new quality measure which reflects the task. In the outset, we will assume $a = 0$, i.e., the ellipsoid is centered at the origin.

Definition 3-6: *Given the set A_β in (3.3-3), the task oriented quality measure $\mu(G)$ of a grasp G is defined as:*

$$\mu(G) = Sup\{\beta \geqslant 0, \text{ such that } A_\beta \subset G(B_1^n \cap K)\} \tag{3.3-4a}$$

i.e., it is the radius of the largest task ellipsoid embedded in $G(B_1^n \cap K)$.

Remark (8): (3.3-4a) applies only to the case when the task ellipsoid is centered at the origin. In the general case the above definition will be modified by offscaling the ellipsoid appropriately.

It is not hard to show that the necessary and sufficient condition for a grasp G to be stable is $\mu(G) > 0$. Unlike the volume measure ν, we do not have unstable grasps with $\mu(G) > 0$.

Let $F(B)$ denote the set of grasps (recall that a grasp consists of k fingers each with only one contact per finger) of a rigid body B. Then, μ is a function

$$\mu: F(\mathrm{B}) \to R_+ \tag{3.3-5}$$

and has the following properties:

(1). It is positively homogeneous:

$$\mu(\lambda G) = \lambda\mu(G), \text{ for all } \lambda \geqslant 0 \tag{3.3-6}$$

(2). It is bi-invariant.

$$\mu(G) = \mu(\tilde{T}G), \tilde{T} \text{ defined in (2.5–6) and } T \in E(3) \tag{3.3-7a}$$

and

$$\mu(G) = \mu(\hat{T}_b G) \text{ for any } b \in R^3 \tag{3.3-7b}$$

Proof.

(1):

$$\mu(\lambda G) = Sup\{\ \beta \text{ such that } A_\beta \subset (\lambda G)(B_1^n \cap K)\ \}$$

$$=Sup\{\beta \text{ such that } \frac{1}{\lambda}A_\beta \subset G(B_1^n \cap K)\}$$

$$=Sup\{\ \beta \text{ such that } A_{(\frac{\beta}{\lambda})} \subset G(B_1^n \cap K)\}$$

$$=Sup\{\lambda\beta' \text{ such that } A_{\beta'} \subset G(B_1^n \cap K\ )\}$$

$$=\lambda\mu(G\,).$$

(2). The proof follows from the definition since both the sets A_β and $G(B_1^n \cap K)$ are transformed by the same transformation matrices. Q.E.D.

In the general case of (3.3-3) when the center of the ellipsoid is located arbitrary in R^6 a similar quality measure $\tilde{\mu}(.)$ is defined below:

$$\tilde{\mu}(G\,) = Sup\{\alpha \text{ such that } A_\beta \subset G(B_{1/\alpha}^n \cap K)\} \tag{3.3-4b}$$

where A_β is one of the sets defined in (3.3-3) with the origin in its interior.

We observe that while the quality measure (3.3-4a) is the largest task ellipsoid can be embedded in the image of $(B_1^n\ \cap K)$ under the grasp G, the quality measure (3.3-4b) is the inverse of the image of the largest ball intersected with K in the domain space that can cover an appropriate task ellipsoid. In the latter definition we let the task ellipsoid contain the origin in its interior so as to guarantee only stable grasps giving nonzero quality measure. Definition (3.3-4a) is both geometrically and computationally simpler, but is not as widely applicable as definition (3.3-4b) because most tasks are not centered at the origin. However, when a task ellipsoid is centered at the origin, it is easy to show that the measures μ and $\tilde{\mu}$ are equivalent, i.e., there exist $K_1, K_2 > 0$ such that

$$K_1\,\tilde{\mu}(G\,) \leqslant \mu(G\,) \leqslant K_2\,\tilde{\mu}(G\,) \;\; \text{for any } G\, \in \tilde{F}(B\,) \tag{3.3-8}$$

The following example illustrates how one can adapt the definition (3.3-4b) to the case where the task is modeled by an arbitrary convex set in T_m^*M.

Example 3-7: Consider again the problem of pencil grasping. Let the task model be given by an open convex set C centered at a point b in $T_m^* M$. The set $\hat{C} = C - b = \{y - b, y \in C\}$ contains the origin in its interior, and $(b + \lambda \hat{C})$, for $\lambda > 0$, rescales the set C. Let $\lambda_o > 0$ be such that $b + \lambda_o \hat{C}$ contains the origin in its interior and define the quality measure of a grasp G by

$$\mu_1(G) = Sup\{\ \alpha, \text{ such that } (b + \lambda_o \hat{C}) \subset G(B^n_{1/\alpha} \cap K)\} \tag{3.3-9}$$

We see that the measure $\mu_1(.)$ also reflects the stability of the grasp G. Furthermore, it satisfies properties (3.3-6) and (3.3-7).

We have introduced three basic quality measures to guide the optimal selection of a grasp. The quality measures δ and ν introduced in sections 3.1 and 3.2 are adequate for either simple tasks or tasks under unknown working environment. These quality measures are easy to compute and are geometrically intuitive. The volume measure ν in some sense may better suit the designer's interest because it is invariant under both body coordinate transformations and change of torque origin. In many applications this property is especially desirable since there is no natural way to specify a body coordinate and a torque origin. Both measures δ and ν do not reflect the task requirement unlike the quality measure μ introduced in this section. The use of the quality measure μ in selecting the optimal grasp will be appreciated better when the task is a sophisticated one and the working environment is partially or completely known. One can then improve one's grasp using the quality measure μ in the selection process.

3.4 Numerical Computation of Quality Measures

In this section, we use some elementary convex analysis to implement the numerical computation of the quality measures defined in (3.1-1), (3.2-1) and (3.3-4). Proofs of some of the standard results studied here may be found in [13]. We first introduce the concept of a support function of a convex set H $\in R^n$.

Definition 3-8: *Let $H \subset R^n$, the support function $\phi(.\,|H): R^n \to R$ of H is defined as*

$$\phi(x\,|H) = Sup\{<x, \tilde{x}>, \tilde{x} \in H\} \tag{3.4-1}$$

Several properties of the support function of a convex set H in R^n are studied in [13]. We quote the following results.

Theorem 3-9: For any two closed convex sets H_1 and H_2 in R^n, $H_1 \subset H_2$ if and only if $\phi(x \mid H_1) \leqslant \phi(x \mid H_2)$ for all $x \in R^n$.

Proof.

See p.113, [13]. Q.E.D.

It follows that a closed convex set H can be expressed as the set of solutions to a system of inequalities given by its support function.

$$H = \{\tilde{x}, <\tilde{x}, x> \leqslant \phi(x \mid H), \text{ for all } x \in R^n\} \tag{3.4-2}$$

Therefore, H is completely determined by its support function, and we have a one-to-one correspondence between closed convex sets in R^n and certain (support) functions in R^n.

The support function of a convex set, specified by a set of linear and quadratic inequality constraints, can be computed numerically by algorithms in [15],[14] & [16]. Using the idea of support functions, we are now ready to compute the quality measure μ of (3.3-4): By theorem 3-9, $A_\beta \subset G(B_1^n \cap K)$ if and only if

$$\phi(x \mid A_\beta) \leqslant \phi(x \mid G(B_1^n \cap K) \quad \text{for } all\ x \in R^n \tag{3.4-3}$$

But the support function of an ellipsoidal convex set A_β is given (see [13], pg. 120) by

$$\phi(x \mid A_\beta) = <-Q^{-1}a, x> + [2\sigma <x, Q^{-1}x>]^{\frac{1}{2}} \tag{3.4-4}$$

where $\sigma = \frac{1}{2} <a, Q^{-1}a> + \beta^2$.

On the other hand, the support function of $G(B_1^n \cap K)$ is,

$$\begin{aligned} \phi(y \mid G(B_1^n \cap K)) &= Sup\{<y, \tilde{y}>, \ \tilde{y} \in G(B_1^n \cap K)\} \\ &= Sup\{<y, Gx>, x \in (B_1^n \cap K)\} \\ &= Sup\{<G'y, x>, \ x \in B_1^n \cap K\} \qquad (3.4\text{-}5) \\ &= \phi(G'y \mid B_1^n \cap K) \end{aligned}$$

Since the support function of the set $B_1^n \cap K$ is readily computable using existing algorithms [15], the calculation of $\mu(.)$ is straight forward by step wise incrementing of β.

In [14], the author described an algorithm that found the nearest distance to a point of a polytope. The polytope may be specified by the convex hull of k points $(p_1, \cdots p_k)$ in a n-dimensional space or by its support function. This algorithm is implemented in [15]. By repeatedly calling this subroutine, one could in principle compute the quality measures δ and ν. We outline a procedure here for calculation of δ (G) for a grasp matrix G together with a force domain K in R^n. Of course, this might not be the most efficient method but it gives the reader an idea on how the computation of these quality measures can actually be performed. First, one computes all (n-1)-dimensional faces of the set $G(B_1^n \cap K)$, and denotes them by $G^c(B_1^n \cap K)$ (See [25] also). Then, one computes for each face the distance of the face to the origin, and denotes it by d_i. The minimum of these d_i's is then the quality measure δ of the grasp G. The calculation of the volume measure ν can be done from its definition and the definition of volume in a general n-dimensional space.

3.5 Optimal Grasp Selection

In this section, we address the problem of maximizing the function $\mu(.)$ over F(B) subject to certain geometric and reachability constraints. For this purpose, we assume that we have: (1). a full geometric description of the rigid body in (3.5-1).

$$\hat{h}_i(x, y, z, c_i) = 0, \text{ for } i = \{1, \cdots l\} \tag{3.5-1}$$

and (2). a complete model of the task and the working environment by a task ellipsoid of the form (3.3-3).

We also assume that the rigid body described by (3.5-1) has a well defined normal almost everywhere, i.e., the set where normals are not defined has an area of measure zero (such as the edges of a cube). Let contact point p_i of ith fingertip (i $\in$ {1, ... k}) belong to contact surface $\hat{h}_{i_j}$ for some $i_j \in$ {1, ... l}, i.e., $\hat{h}_{i_j}(p_i, c_{i_j}) = 0$. Notice that the index i stands for the ith finger while the index i_j stands for the $i_j th$ surface. At a point p_i where the normal is well defined let the unit normal to the contacting surface

$\hat{h}_{i_j}$

be denoted by $f_1^i(p_i)$. namely

$$f_1^i(p_i) = \frac{\nabla h_{i_j}(p_i)}{||\nabla h_{i_j}(p_i)||} \tag{3.5-2}$$

Also, let the two unit tangent vectors to h_{i_j} at p_i be denoted by $f_2^i(p_i)$ and $f_3^i(p_i)$, which determine along with $f_1^i(p_i)$ an orthonormal basis at point p_i. Let $m_4^i(p_i) = f_1^i(p_i)$ for a soft finger contact, we write explicitly the dependence of the grasp matrix G on the contact configuration $(p_i)_{i=1}^{i=k}$ as

$$G = \begin{bmatrix} f_1^1(p_1) & \cdots & f_3^1(p_1), & \cdots & f_3^k & 0 \\ f_1^1(p_1)\times(p_1-o) & \cdots & f_3^1(p_1)\times(p_1-o) & \cdots & f_3^k\times(p_k-o) & m_4^k(p_k) \end{bmatrix} \tag{3.5-3}$$

For i = {1, ... k}, the point p_i belongs to the surface h_{i_j} and consequently satisfies one of the (3.5-1) constraints. By composing the function G with μ, we obtain an new function $\overline{\mu}$: $R^{3k} \rightarrow R$ from the parameter space $p_i = (p_x^i, p_y^i, p_z^i)$, i = {1, ...k} into the reals R given by $\overline{\mu} = \mu\,(G)$.

The problem of optimal grasping is then the problem of

$$\underset{\{(p_1,\ldots p_k)\in R^{3k}\, h_{i_j}(p_i,c_{i_j})=0\}}{Maximize} \quad \overline{\mu}(p_1,p_2,p_3,\cdots p_k) \tag{3.5-4}$$

a constrained optimization problem.

The function $\overline{\mu}$ may be non-differentiable with respect to its argument $p_i = (p_x^i, p_y^i, p_z^i)$ and the solution of (3.5-4) is often called a non-differentiable optimization problem. Heavy computation is usually involved, but efficient algorithms are being developed in literature ([16]).

Example 3-10: We conclude this section with an example of a two-fingered grasp of a rectangular planar object. The object shown in Figure 7 has weight c and is obtained by intersecting four half planes. We will assume that the task ellipsoid is a ball in R^3, i.e.,

$$A_\beta = \left\{ (f_x, f_y, \tau_z) \in R^3, \ f_x^2 + (f_y - c)^2 + \tau_z^2 \leq \beta^2 \right\} \tag{3.5-5}$$

where f_x, f_y, and τ_z are respectively magnitudes of the linear forces along the x- and y-directions and magnitude of the torque about "o" along the z-direction. We are asked to find a grasp which is optimal with respect to the task specified in (3.5-5).

Let the planar object in the figure be specified by a function

$$h = h(x, y) = 0 \tag{3.5-6}$$

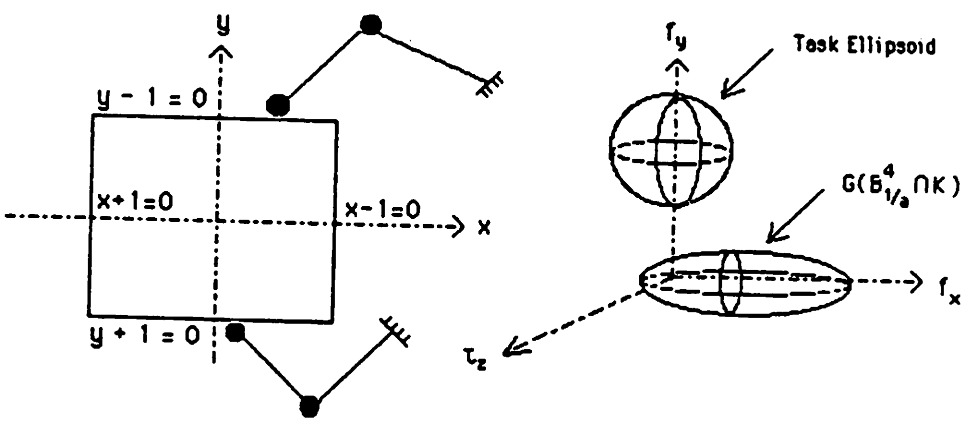

Figure 7. Two-fingered planar grasping.

The unit normal to the surface of (3.5-6) at a point p_i, $i = \{1, 2\}$, is given by

$$f_1^i(p_i) = \frac{\nabla h(p_i)}{\|\nabla h(p_i)\|} = \nabla \tilde{h}(p_i) = \begin{Bmatrix} \dfrac{\partial \tilde{h}(p_i)}{\partial x} \\ \dfrac{\partial \tilde{h}(p_i)}{\partial y} \end{Bmatrix} \tag{3.5-7}$$

where the symbol "~" denotes normalized quantities. The unit tangent vector to (3.5-6) is

$$f_2^i(p_i) = \begin{bmatrix} \dfrac{\partial \tilde{h}(p_i)}{\partial y} \\ -\dfrac{\partial \tilde{h}(p_i)}{\partial x} \end{bmatrix} \tag{3.5-8}$$

We observe that the tangent and normal vectors to the object are well defined everywhere except at the corners. We will not consider points which have no well defined tangent or normal vector as grasping locations. The resulting torques of $f_1^i(p_i)$ and $f_2^i(p_i)$ about the origin are

$$m_1^i(p_i) = p_y^i \frac{\partial \tilde{h}(p_i)}{\partial x} - p_x^i \frac{\partial \tilde{h}(p_i)}{\partial y} \tag{3.5-9}$$

$$m_2^i(p_i) = p_y^i \frac{\partial \tilde{h}(p_i)}{\partial y} + p_x^i \frac{\partial \tilde{h}(p_i)}{\partial x} \tag{3.5-10}$$

Assuming that both contacts are point contacts with friction, the grasp matrix G : $R^4 \rightarrow R^3$ is

$$G = \begin{bmatrix} f_1^1(p_1) & f_2^1(p_1) & f_1^2(p_2) & f_2^2(p_2) \\ m_1^1(p_1) & m_2^1(p_1) & m_1^2(p_2) & m_2^2(p_2) \end{bmatrix} \tag{3.5-11}$$

The force domain K $\in R^4$ is given by

$$K = \{x \in R^4, x_1 \geqslant 0, x_2^2 \leqslant \mu_1^2 x_1^2, x_3 \geqslant 0, x_4^2 \leqslant \mu_2^2 x_x^2\} \tag{3.5-12}$$

To balance any external wrench $(f_x, f_y, t_z)^t$, the applied finger force $x \in R^4$ must satisfy

$$\begin{bmatrix} f_x \\ f_y \\ \tau_z \end{bmatrix} = G \begin{bmatrix} x_1 \\ x_2 \\ x_3 \\ x_4 \end{bmatrix} \tag{3.5-13}$$

If we can find such an x in K that solves (3.5-13), then static equilibrium is possible. For example, when $(f_x, f_y, \tau_z) = (0, c, 0)$, one solution would be $p_1 = (0, -1)$, $p_2 = (0,1)$, $x_i = 0$ for $i > 1$ and $x_1 = c\{\frac{\partial \tilde{h}(p_1)}{\partial y}\}^{-1}$.

Even for such a two dimensional example, the solution to (3.5-4) requires heavy computation. But we can give a qualitative description of the set $G(B^4_{\frac{1}{\alpha}} \cap K)$. Apparently, the contact point (p_1, p_2) must not lie on the same edge to achieve stable grasp. The four candidate grasping pairs left are

$$I.\ p_1 = (0, -1), p_2 = (0, 1); \qquad II.\ p_1 = (1, 0), p_2 = (-1, 0) \tag{3.5-14}$$

$$III.\ p_1 = (0, -1), p_2 = (-1, 0); \qquad IV.\ p_1 = (0, 1), p_2 = (1, 0)$$

Since the task ellipsoid shown in the figure is located right above the f_y axis, a "good" grasp should have the image set $G(B^4_1 \cap K)$ oriented in the f_y direction. Any grasp whose image set $G(B^4_1 \cap K)$ oriented along other directions is considered an inefficient grasp because the applied body wrenches are not in the range of required task forces. The first grasping pair (I) has the set $G(B^4_1 \cap K)$ oriented along the direction of the task ellipsoid and obviously achieves a better quality measure. The image ellipsoid of grasping pair (II) would have identical shape as grasping pair (I) but oriented along the f_x direction. As far as this particular task is concerned it is not the optimal choice. The reader can readily verify that the other two grasping pairs do not achieve higher quality measures than grasping pair (I). Notice that the difference between grasp pairs (I) and (II) becomes insignificant as weight of the object is reduced.

3.5.1 Additional Constraints and Fine Manipulation

Additional constraints beside the geometric constraints (3.5-1) to be considered are *reachability constraints* and *hand constraints*.

Reachability constraints as considered in [10] include accessibility of the hand to the target object, and obstacles in the working environment. For example, when an oddly shaped object as shown in Figure 8 is sitting on top of a table, then face A, B, C and D are not accessible by a robot hand.

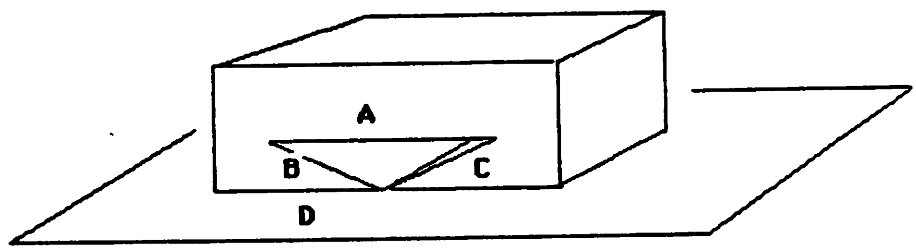

Figure 8. An oddly shaped object on a table

While constraints on face A, B and C could be classified as intrinsic constraints, the constraint on face D is extrinsic and could be eliminated if we turn the object around (and create new constraints). There are also other types of constraints dependent upon the environment and the object shape. See [10] for further discussions of reachability constraints.

Hand constraints often refer to constraints imposed by geometry, working volume of the hand and spreading distances of each finger. Without loss of generality, we may assume these constraints considered are given by

Reachability constraints:

$$\tilde{h}_j(p_i, \hat{c}_j) \neq 0; \text{ for all } i = \{1, \cdots k\}, \text{ and some } j = \{1, \cdots p\} \qquad (3.5\text{-}15)$$

Hand constraints:

$$\tilde{g}_j(p_1, \cdots p_k, d_1, \cdots d_{l_j}) = 0, \quad j = \{1, \cdots \tilde{p}\} \qquad (3.5\text{-}16)$$

where the constants ($\hat{c}_j$, d_i, p and $\tilde{p}$) come from the constraints.

Hence, we have p reachability constraints and $\tilde{p}$ hand constraints. The optimization problem (3.5-4) is done subject to a total of $(k + p + \tilde{p})$ constraints. The amount of computation time goes up with the number of constraints.

Recent advances in dextrous hand design ([23]) enables fine motion of the object within the robot hand ([6], [7]). Therefore, some of the reachability constraints (3.5-15) may be eliminated by performing a fine motion of the object in the hand. For example as in Figure 7, while face D is not reachable at the initial grasping configuration it can be reached once the object is picked up from the table and a better grasping configuration may be obtained. Human hands perform such operations frequently; when one grasps a pencil, one would first pick up the pencil and then manipulate it around in the hand to get to the final grasping configuration which is optimal to execute the task. Of course, in robot applications, such an operation is limited by the fine motion manipulability of the robot hand.

3.6 Dynamic Grasping

As we can see from (3.3-4) that the quality measure of a grasp depends heavily on the specific task to perform. As the task varies, the measure of a grasp may change dramatically. A grasp which is optimal for one task may be completely different for another. The process of updating the grasp in response to changed task ellipsoid is called dynamic grasping. Dynamic grasping happens on many occasions. When a cup is filling with water, the weight of the cup increases with time and the task ellipsoid varies. We observe that the corresponding action of the human hand is to move up the finger so as to keep the grasp optimal.

Also when a target object in compliant motion is moved from one environment into another, the disturbance ellipsoid may change significantly and updating the original grasp becomes necessary in order to carry out the task. Dynamic grasping is closely associated with the ability of the robot hand in imparting fine motions. Nevertheless, dynamic grasping is a very interesting problem both theoretically and application wise. We will discuss these issues in latter papers.

4. Suggestion for Future Work

We studied in this paper the problem of optimal grasping by a multifingered robot hand. The optimality criteria were based on some quality measures defined in Section 3. Since all these measures are directly or numerically computable the problem of optimal grasping can be attacked. The numerical issues associated with optimal grasping have not however been completely discussed and our future effort will study these problems in greater detail.

As we can observe from human grasping experience, the assumption made of one contact per finger at the finger tip is rather strict and inpractical. Very often, human hands rely on contacts at finger links and at hand palm as well to achieve a *good* grasp. With only one contact per finger, the set of achievable grasps is precision grasp and a large class of other grasps studied in [6] such as power, lateral grasps can not be achieved. Consequently, it is important to relax this assumption and extend the study of optimal grasping. Further it follows that dimension of the force domain K is also an optimization variable as well as the contacting configuration for each fixed K. The dimension of this force domain may get very large as multiple contacts are allowed.

Human grasping experience tells us, when one grasps a light object to perform tasks which require low-level forces, one usually select grasps that have small number of contacts; when one grasps a heavy and large object or a light object to perform tasks which require high-level forces one selects grasps with large number of contacts. Such grasps are usually called redundant grasps or power grasps. The question that then arises is: given a specific task to perform, what is the optimal number of contacts and their contacting locations? Namely, given two grasps

$$G_1: R^{12} \rightarrow T_m^* M \tag{4-1}$$

$$G_2: R^{36} \rightarrow T_m^* M \tag{4-2}$$

with associated force domains $K_1 \subset R^{12}$ and $K_2 \subset R^{36}$ and a common task to perform, how does one compare the quality of the two grasps? Consider again the pencil grasping example. Suppose that two grasps are given as above, while G_1 corresponds to a regular human dextrous grasp with 4 contacts, G_2 is a power grasp with 12 contacts. Apparently, it might be true that $\mu(G_2) \geqslant \mu(G_1)$, but a human always selects grasp G_1 because it gives not only better manipulatability but also better senstivity. On the other hand if the pencil is a Chinese brush pen (usually heavy and large) then grasp

G_2 may be chosen instead.

The theory developed so far is still not adequate to answer the question of how physical properties (weight, shape, size, etc) of an object and task requirement determine not only the grasping locations but also the *number of contacts of a grasp*. But it does present some approaches to the problem.

Acknowledgements

This work is supported by NSF PYI Grant #DMC-8451129. We would like to thank Drs. Robyn Owens, Brad Paden, and Mr. John Hauser, Paul Jacobs and Greg Heinzinger for their critical and useful comments.

References:

[1] Brady, M., et al, *Robot Motion Planning and Control*, MIT Press, 1983.

[2] R. Paul, *Robot Manipulators: Mathematics, Programming, and Control*, MIT Press, 1981.

[3] Hanafusa, H. & Asada, H. "Stable prehension by a robot hand with elastic fingers", Proc. 7th ISIR, Tokyo, Japan, 1977, pp.361-368.

[4] Asada, H. "A robotic hand with elastic fingers and its application to assembly process", Proc. of IFAC Symp. on Information Control Problem in Production Engineering 1977, pp.127-138.

[5] Salisbury, J. K., "Kinematic and force analysis of articulated hand", Ph.D. thesis, Stanford Univ. Dept. of Mechanical Eng. May 1982.

[6] Cutkosky, M.R., "Grasping and fine manipulation for automated manufacturing ", Ph.D. Thesis, Carnegie-Mellon Univ. Dept. of Mechanical Eng. Jan. 1985.

[7] Kerr, J., "An analysis of multifingered hand", Ph.D. Thesis, Stanford Univ. Dept. of Mech. Eng., Dec. 1984.

[8] Holzman, W. and McCarthy, J. M., "Computing the friction forces associated with a three fingered hand", *IEEE Journal of Robotics and Automation*, Dec. 1985, pp.206 -210.

[9] Jameson, J., "Analytic techniques of automated grasp", Ph.D. Thesis, Stanford

Univ. Dept. of Mech. Eng. June, 1985.

[10] Lozano-Perez, T., "Task planning", in *Robot Motion Planning and Control* Cambridge, MA: MIT Press, 1982, pp. 473-498.

[11] Bottema, O. and Roth, B., *Theoretical Kinematics*, North-Holland Publishing Company, 1979.

[12] Paden, B., "Kinematics and Control of Robot Manipulators", Ph.D. Thesis, Univ. of California, Berkeley. Dept. of EECS, May 1985.

[13] Rockafellar, R.T., *Convex Analysis*, Princeton Mathematics Series, Vol. 28, Princeton Univ. Press, 1970.

[14] Wolfe, P., "Finding the nearest point in a polytope", *Mathematical Programming*, (1976) pp. 128-149.

[15] Hauser, J., "Proximity algorithms: Implementation and Applications", M.S. Project, Univ. of California, Berkeley. Dept. of EECS, May 1986.

[16] Polak, E., *Computational Methods in Optimization*, Academic Press, 1971.

[17] Boothby, W., *An Introduction to Differentiable Manifolds and Riemannian Geometry*, Academic Press, 1975

[18] Abraham, R. and Marsden, J., *Foundations of Mechanics*, Benjamin / Cummings Publishing Company, 2nd ed. 1978.

[19] Wolter, J. D., Volz, R. A., and Woo, A.C., "Automatic generation of gripping position", *IEEE Trans. on Systems, Man, and Cybernetics*, Vol. SMC-15, No.2, pp.204-213, March/April 1985.

[20] Barber, J. and Volz, R. A., etc, "Automatic two-fingered grip selection", IEEE Int'l Conf. on Robotics and Automation, pp.890-896, April 1986.

[21] Peshkin, M. and Sanderson, A., "Reachable grasps on a polygon: The convex rope algorithms", *IEEE Journal on Robotics and Automation*, Vol. RA-2, No. 1, March 1986.

[22] Loncaric, J., "Geometrical Analysis of Compliant Mechanism in Robotics", Ph.D. Thesis, Harvard University, Division of Applied Sciences, May 1985.

[23] Jacobsen, S. C., Wood, J. E., Knutti, D. F., and Biggers, K.B., " The Utah/MIT Hand: Work in Progress" in *Robotics Research* edited by M. Brady & R. Paul, MIT Press 1984.

[24] Goldstein, H. *Classic Mechanics*, 1980 2nd Edition, Addison-Wesley, Reading

Mass.

[25] Yoshikawa, T., "Manipulability of Robotic Mechanism", Technical Report, Kyoto University, Uji, Kyoto 611, Japan.